都市ヒートアイランドの経年変化評価のための 名古屋市の夏季 Landsat LST データの解析

エイ タンダー ウェ*・谷口 健太・高田 雄登***・松原 芽衣***・ 岡田 征太郎***・内田 主税*****

Summer Landsat Land Surface Temperature Analysis for Urban Heat Island Trend Assessment in Nagoya, Japan

Aye Thandar Wai*, Kenta Taniguchi**, Yuto Takada***, Mei Matsubara***, Seitaro Okada***, Chikara Uchida*****

Abstract: This study analyzed summer seasonal Landsat-derived land surface temperature (LST) trends over a 40-year period (1986-2025) at subway stations in Nagoya City, Aichi Prefecture, Japan, to evaluate long-term patterns of the surface urban heat island (SUHI) effect. The analysis utilized the Collection 2 Level-2 Science Product (L2SP), in which LST images are atmospherically corrected and resampled to a 30 m resolution. Numerical experiments were conducted to investigate the spatiotemporal behavior of summer LST anomaly percentiles within 1 km buffer zones around selected subway stations. The results revealed shifts in the inter-station relationships of summer LST anomalies. These findings suggest that geospatial processing of L2SP data provides reliable metrics for assessing local SUHI intensification at the neighborhood scale (approximately 1 km) under mid-morning conditions.

Keywords: ランドサット（Landsat），都市ヒートアイランド（Urban Heat Island），地表面温度（Surface Temperature），公共交通指向型開発（Transit-Oriented Development, TOD），名古屋市（Nagoya City）

1. Introduction

Global warming affects land cover not only through glacial degradation but also by intensifying the urban heat island (UHI) effect. Urban planning plays a significant role in mitigating and adapting to these ongoing changes. One promising approach is the development of a smart urban environment based on the concept of transit-oriented development (TOD), although the effectiveness of this strategy largely depends on the quality of TOD designs (Kamruzzaman et al., 2018).

For example, the subway transport system in Nagoya City, Aichi Prefecture, Japan, indirectly contributes to UHI mitigation as its four lines support compact, walkable urban design and reduce reliance on private vehicles. Accordingly, monitoring UHI across various subway stations provides an effective means of assessing UHI within the framework of the TOD concept. Numerous studies have examined surface UHI (SUHI) using vertical temperature profiles based not only on air temperature but also land surface temperature (LST) (Tremeac et al., 2012; Wong et al., 2021), and both daytime and nighttime SUHI trends in Nagoya City have been investigated (Hisatsune, 2023). Previous research also demonstrated the utility of remotely sensed LST imagery from the Japanese GCOM-C satellite in capturing SUHI patterns in the city.

A long-term perspective is essential for gaining a deeper understanding of SUHI phenomena in megacities that have undergone continuous urbanization over decades. By processing LST imagery from Landsat satellites available since 1972, we can access a rich archive of historical data that provides valuable insights into SUHI dynamics. Among the Landsat data products for surface analysis, the Collection 2 Level-2 Science Product (L2SP) is particularly useful, as it provides atmospherically corrected LST imagery resampled to a 30 m resolution.

Taniguchi et al. (2023) employed summer seasonal LST data cubes from L2SP over glacial mountain regions, assuming spatial homogeneity in snow and ice cover, to visualize decadal trends in glacial shrinkage during summer. This suggests the possibility of extending the procedure to other applications, such as SUHI monitoring, which is urgently needed to address increasing thermal stress in summer. Unlike glacial

* 非会員 日本工営都市空間株式会社 技術本部 DX 推進室（Nippon Koei Urban Space Co., Ltd.）
〒461-0005 愛知県名古屋市東区東桜 2-17-14 新栄町ビル E-mail：b1380@n-koei.co.jp
** 正会員 日本工営都市空間株式会社 技術本部 DX 推進室
*** 非会員 日本工営都市空間株式会社 総合調査コンサルタント事業本部
**** 非会員 日本工営都市空間株式会社 都市開発コンサルタント事業本部

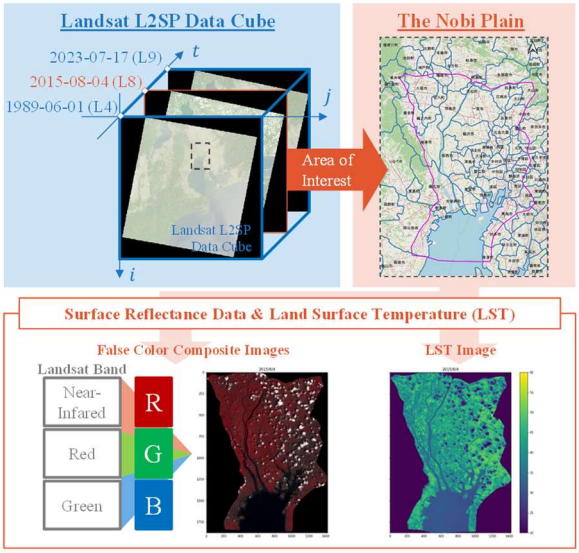


Figure 1 Illustration of Landsat L2SP-based false color composite and LST images over the Nobi Plain, Japan.

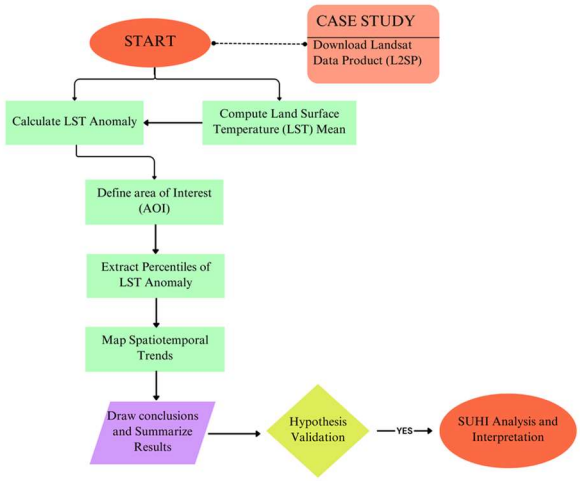


Figure 2 Workflow diagram of the methodology used in this study for surface urban heat island (SUHI) analysis.

environments, however, the urban spaces surrounding subway stations are highly heterogeneous. Therefore, this study adapts the earlier methodology to SUHI analysis using a geographical information system (GIS). The objective of this paper is to analyze summer seasonal Landsat-derived LST trends at subway stations in Nagoya City to evaluate the SUHI dynamics from a long-term perspective.

2. Data

This study uses L2SP, which provides varied remotely sensed imagery acquired via sensors onboard Landsat satellites. Within L2SP, LST imagery is available after atmospheric correction, with a spatial resolution resampled to 30 m, whereas the original resolution is 100 m. The LST imagery from L2SP is particularly suitable for visual comparison with other spectral bands. Figure 1 illustrates a false-color composite image composed of near-infrared, red, and green bands together with LST over the Nobi Plain, as observed by Landsat-8 on August 4, 2015. The Nobi plain is well known as a low-lying plateau region, and the L2SP scenes used correspond to Path 109 and Row 31, with a scene center time of approximately 10:28 a.m. in JST. In Figure 1, areas shown in red are zones of high vegetation greenness, while white areas indicate clouds present at the time of observation. These clouds, which can be visually identified, correspond to regions with low LST. To address this issue, this study adopts metrics designed to minimize the effects of cloud contamination in SUHI analysis.

3. Method

A simplified procedure was developed to process LST data by extending the approach proposed in Taniguchi et al. (2023). The overall workflow consisted of five steps, as illustrated in Figure 2.

First, we considered a time series of LST images, represented as $M \in \mathbb{R}^{n_j \times n_i \times n_t}$, with n_j and n_i denoting the number of pixels along the Y- and X-axes, respectively, and n_t representing the number of temporal scenes. Second, the LST value at the spatial coordinates (i,j) and time t, denoted as $m_{i,j,t}$, was converted into the LST anomaly $m'_{i,j,t}$ using the following equation:

$$m'_{i,j,t} = m_{i,j,t} - \hat{\mu}_{i,j} \quad (1)$$

where $\hat{\mu}_{i,j}$ is the mean values of LST at location (i,j), calculated exclusively from cloud-free scenes. The exclusion of cloudy scenes was essential to establish a reliable baseline for anomaly computation.

Third, the anomaly images were cropped to polygons generated as buffer zones around the geographical coordinate point $\boldsymbol{p}_x$ of each subway station x in the Nagoya subway network. Fourth, from the 30 m Landsat LST data cropped by the buffer around $\boldsymbol{p}_x$, the percentile value m was extracted. In this study, the percentile value at time t was defined as $v_{x,m}(t)$. Finally, in the fifth step, the percentile data $v_{x,m}(t)$ were interpreted and compared between pairs of stations. For stations x and y, the difference in percentile values was calculated as

$$\delta v_{x,y,m}(t) = v_{x,m}(t) - v_{y,m}(t). \quad (2)$$

4. Numerical Experiments

A series of numerical experiments was conducted using Quantum GIS (QGIS) software. In this environment, buffer

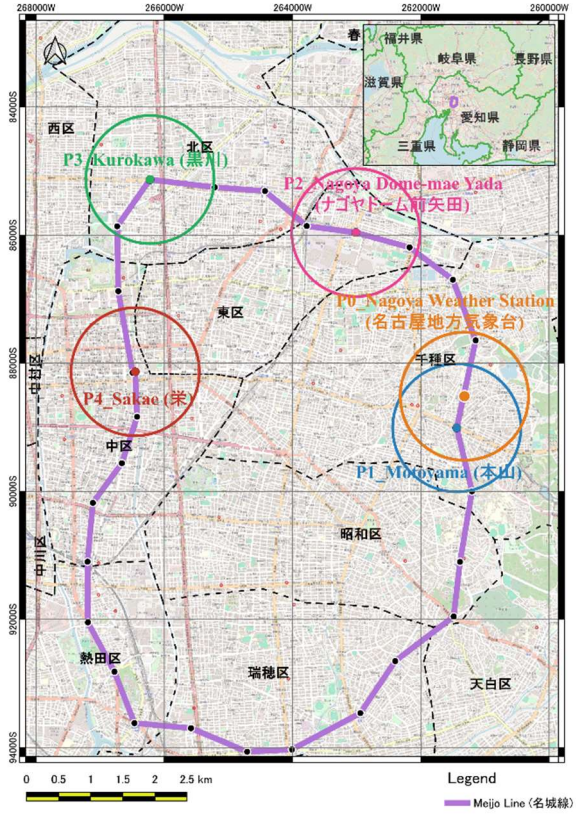


Figure 3 Maps showing 1-km buffers around weather station (p_0) and subway stations (p_1-p_4) in QGIS.

zones were generated with their centers located at each station point p_x. In this study, the radii of all buffers were set to 1,000 m. Percentile values of LST anomalies were then mapped and compared across the individual buffer zones.

A total of 39 L2SP values from 1986 to 2025 were downloaded, covering the summer months of June, July, and August under conditions of less than 20 percent cloud coverage, representing clear-sky conditions. After visual inspection to exclude residual cloud contamination, 26 scenes were selected to construct the LST cube for baseline estimation. The LST baseline for the 1986-2025 summer period was then derived from this cube, and individual LST anomalies were calculated accordingly.

In addition to L2SP, a time series of air temperature data recorded at the Nagoya weather station p_0 was collected. Figure 3 provides an overview of the spatial distribution of station locations from p_0 to p_4. To compare LST trends with air temperature, statistical measures—minimum, mean, and maximum—were computed for the three summer months of each year. These summer air temperature records were obtained from the Japan Meteorological Agency (JMA), which operates under the Ministry of Land, Infrastructure, Transport and Tourism (MLIT).

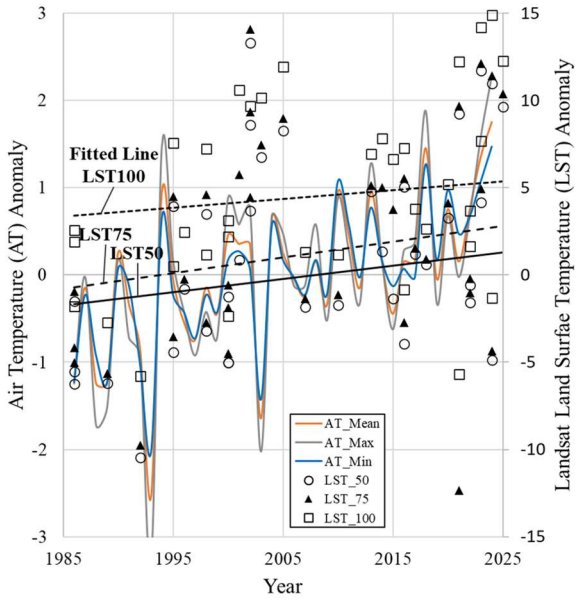


Figure 4 Air temperature (AT) and land surface temperature (LST) anomalies at p_0.

5. Results

5.1 LST anomaly at Nagoya weather station

Two types of temperature anomalies relative to the 1986-2025 summer baseline at Nagoya weather station (p_0) are plotted in Figure 4. The first is the air temperature anomaly, where the minimum, mean, and maximum values are shown as blue, orange, and gray lines, respectively. The second is the LST anomaly, represented by three-level percentiles $v_{0,m}$. As shown in Figure 4, both air temperature and LST anomalies exhibit increasing trends. The magnitude of the air temperature anomaly at the Nagoya weather station ranges from approximately 2-3 °C, whereas the LST anomaly derived from Landsat imagery exceeds 10 °C. Notably, the percentiles of individual LST anomalies also show a positive trend.

The distribution of percentile values indicates that higher LST anomalies are concentrated during 2000-2005 and 2020-2025. In contrast, the preceding five-year intervals (1995–2000 and 2015–2020) exhibit slightly cooler anomalies. This pattern suggests the presence of decadal-scale fluctuations in summer LST anomalies around the Nagoya weather station.

5.2 Comparison among stations

Figure 5 presents the differences $\delta v_{0,1,m}$ for three percentiles $(m = 50, 75, 100)$, plotted as a circle, triangle, and square, respectively. These anomaly differences reveal biases that emerge among the distinct buffer spaces. The fitted lines shift upward with an increase in percentile m, indicating that the area surrounding station p_1 exhibits relatively lower LST anomalies compared with those at the weather station p_0.

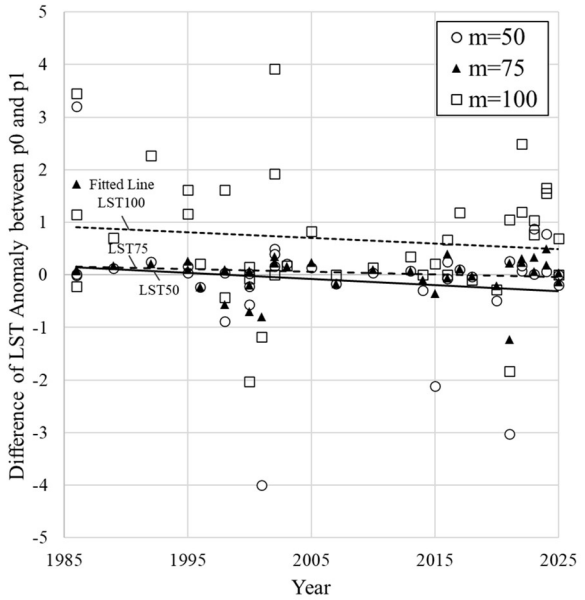


Figure 5 Plots of difference $\delta v_{0,1,m}$ for the pair p_0-p_1.

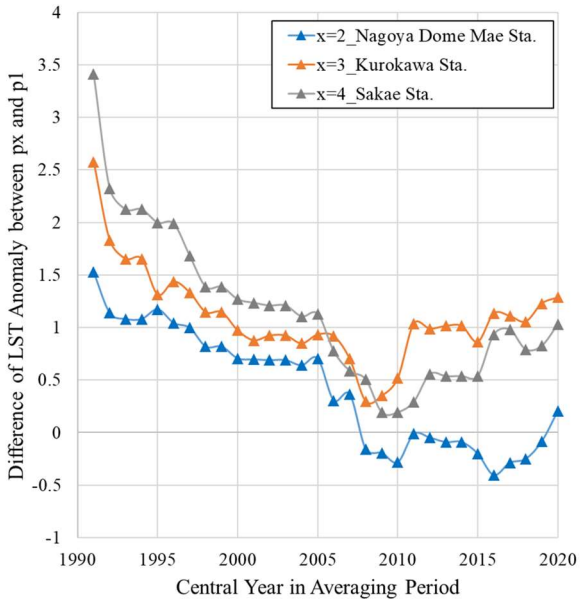


Figure 6 Plots of the 11-year average of $\delta v_{x,1,75}$.

Since the buffer at p_0 includes varied land cover types, such as grasslands, lakes, hills, buildings, and roads, the LST anomaly around p_0 exhibits complex variability. In addition to these land cover dependencies, another major factor arises from the relationship between building geometry and solar incidence, which produces shading effects. For example, around point p_1, major roads are surrounded by high-rise buildings. It is, therefore, assumed that building shadows extend across wide areas and contribute to a reduction in LST prior to noon.

Finally, the inter-station relationship of LST anomalies at the 75th percentile relative to p_1 was examined (Figure 6). The smoothed lines in the figure were obtained by averaging $\delta v_{x,1,75}$ over an 11-year moving window, excluding values of $\delta v_{x,1,m}$ less than -2.0°C. Two distinct relative trends were identified: one for the station pair p_1-p_2 and another for the pairs p_1-p_3 and p_1-p_4. Interestingly, the relative differences tended to increase with the number of stations away from p_1 until around 2010. After 2010, however, the trends diverged: some continued to increase, while others stabilized. These findings imply notable changes in the inter-station relationship of summer LST anomalies during mid-morning periods.

These findings suggest that geospatial processing of L2SP provides suitable metrics for assessing local SUHI intensification at the 1 km scale during mid-morning. Further research is required to integrate and inter-calibrate these results with geostationary satellites, such as Himawari-8, to capture SUHI dynamics from both daily and annual perspectives.

6. Summary

This study introduced a procedure for deriving Landsat L2SP-based LST anomalies and analyzed summer seasonal LST trends over a 40-year period (1986-2025) at subway stations in Nagoya City to evaluate long-term trends in the surface urban heat island (SUHI) effect. The procedure was designed to obtain anomaly trends by combining buffering around weather and subway stations. The results revealed slight differences among station percentiles, likely attributable to surface characteristics such as building heights and urban morphology. Moreover, changes in the inter-station relationships of LST anomalies were observed during summer mid-morning periods. Overall, this study demonstrates that geospatial processing of L2SP can provide robust metrics for evaluating local SUHI intensification at the 1 km scale during mid-morning.

References

久恒邦裕（2023）人工衛星を用いた名古屋市の地表面温度の測定.「名古屋市環境科学調査センター年報」, 12, 12-16.

Kamruzzaman, M., Deilami, K., and Yigitcanlar, T. (2018) Investigating the urban heat island effect of transit oriented development in Brisbane. *J. Transp. Geogr.*, **66**, 116-124.

Taniguchi, K., Sugiyama, T., Uchida, C., Sano, S., Obata, K., and Yoshioka, H. (2023) Investigation of the smoothed peak NDVI trend over Tsambagarav national park based on Landsat time series data. *Proc. JpGU2023*, ACG36-P06. (abstract only)

Tremeac, B., Bousquet, P., de Munck, C., Pigeon, G., Masson, V., Marchadier, C., and Meunier, F. (2012) Influence of air conditioning management on heat island in Paris air street temperatures. *Appl. Energy*, **95**, 102-110.

Wong, N., Tan, C., Kolokotsa, D., and Takebayashi, H. (2021) Greenery as a mitigation and adaptation strategy to urban heat. *Nat. Rev. Earth Environ.*, **2**(3), 166-181.